

Mixed dark matter from technicolor

Alexander BELYAEV*

*NExT Institute: School of Physics & Astronomy, Univ. of Southampton, UK
Particle Physics Department, Rutherford Appleton Laboratory, UK*

Mads T. FRANSEN and Subir SARKAR†

Rudolf Peierls Centre for Theoretical Physics, University of Oxford, UK

Francesco SANNINO‡

CP³-Origins, University of Southern Denmark, Odense M, DK

We study natural composite cold dark matter candidates which are pseudo Nambu-Goldstone bosons (pNGB) in models of dynamical electroweak symmetry breaking. Some of these can have a significant thermal relic abundance, while others must be mainly asymmetric dark matter. By considering the thermal abundance alone we find a lower bound of m_W on the pNGB mass when the (composite) Higgs is heavier than 115 GeV. Being pNGBs, the dark matter candidates are in general light enough to be produced at the LHC.

I. INTRODUCTION

A second strongly coupled sector in Nature akin to QCD is a likely possibility. The new strong interaction may naturally break the electroweak (EW) symmetry through the formation of a chiral condensate, thus making the Standard Model (SM) Higgs a composite particle. Models of this type are called ‘technicolor’ (TC) [1, 2] and several new variants have been proposed recently [3–11] with interesting dynamics relevant for collider phenomenology [12–15] as well as cosmology [10, 16–36]. A review of these models and the phase diagram of strongly coupled theories can be found in Ref. [37]. A relevant point is that the technicolor dynamics is strongly modified by the new interactions necessary to give masses to SM fermions [38] and the interplay between these two sectors leads to an entirely new class of models, constraints on which were discussed in Ref. [39].

We discuss different possibilities for dark matter (DM) candidates within this rich framework and show that some of these composite states can be thermal relics while being sufficiently light to be produced at the LHC.

We call dark matter candidates composed of technicolor fields ‘technicolor interacting massive particles’ (TIMPs) and focus on those which are pseudo Nambu-Goldstone bosons (pNGB). Our analysis is general since we use a low energy effective description for the TIMPs which can easily be adapted for specific models. We will discuss some of these models [8, 10, 20, 30] which provide particularly interesting candidates for dark matter.

II. THE SIMPLEST TIMPs FROM PARTIALLY GAUGED TECHNICOLOR

An interesting class of TIMPs arise from *partially gauged technicolor* models [6, 40] in which only part of the TC group is gauged under the EW interactions. The EW gauged technifermions are organized in doublets in the usual way while the other technifermions are collectively denoted λ^f , with f counting these flavors only:

$$Q_L = \begin{pmatrix} U_L \\ D_L \end{pmatrix}, U_R, D_R; \lambda^f \quad (1)$$

These models were introduced originally in order to yield the smallest naïve EW S parameter, while still being able to achieve walking dynamics.¹ The non-minimal flavor symmetry of the resulting model allows for a number of light states accessible at colliders. A similar scenario is envisaged in so-called *conformal technicolor* [43, 44]. The technifermions not gauged under the EW interactions essentially constitute a strongly interacting *hidden sector*.

To be specific we consider a scalar TIMP, $\phi \sim \lambda\lambda$, made of the SM gauge singlet technifermions λ^f and possessing a global $U(1)$ symmetry protecting the lightest state against decay. Moreover we take ϕ to be a pNGB from the breaking of chiral symmetry in the hidden sector, which leaves this $U(1)$ unbroken. This constitutes the simplest type of TIMP from the point of view of

¹ The naïve S -parameter from a loop of technifermions counts the number of fermion doublets transforming under weak $SU(2)_L$, while walking dynamics is required to reduce non-perturbative contributions to the full S -parameter. The naïve S -parameter has recently been conjectured to be the absolute lower bound of the full S -parameter [41, 42], making the TC models presented here optimal with respect to satisfying the LEP precision data.

*Electronic address: a.belyaev@phys.soton.ac.uk

†Electronic address: m.frandsen1@physics.ox.ac.uk

‡Electronic address: sannino@cp3.sdu.dk

its interactions so we study this first and consider later TIMPs with constituents charged under the SM. An explicit model of partially gauged technicolor featuring this kind of TIMP is ‘ultra minimal technicolor’ (UMT) [8]. We therefore identify our DM candidate with a complex scalar ϕ , singlet under SM interactions and charged under a new $U(1)$ symmetry (*not* the usual technibaryon symmetry), which makes it stable.

In addition to the TIMP we consider a light (composite) Higgs boson. A general effective Lagrangian to describe this situation is presented below and can be derived, for any specific model, from the UMT Lagrangian [8]. At low energies we can describe the interactions of ϕ through a chiral Lagrangian. The (composite) Higgs H couples to the TIMP as:

$$\begin{aligned} \mathcal{L} = & \partial_\mu \phi^* \partial_\mu \phi - m_\phi^2 \phi^* \phi + \frac{d_1}{\Lambda} H \partial_\mu \phi^* \partial_\mu \phi \\ & + \frac{d_2}{\Lambda} m_\phi^2 H \phi^* \phi + \frac{d_3}{2\Lambda^2} H^2 \partial_\mu \phi^* \partial_\mu \phi + \frac{d_4}{2\Lambda^2} m_\phi^2 H^2 \phi^* \phi. \end{aligned} \quad (2)$$

The interactions between technihadrons such as ϕ made of EW singlet constituents and states with EW charged constituents (e.g. H) are due mainly to TC dynamics and, as such, the couplings between these two sectors are *not* suppressed [8]. However, since ϕ is a pNGB it must have either derivative couplings or the non-derivative couplings must vanish in the limit $m_\phi \rightarrow 0$. The mass m_ϕ is assumed to come from interactions beyond the TC sector, e.g. ‘extended technicolor’ (ETC) [45, 46] which can provide masses for the TC Nambu-Goldstone bosons, as well as for SM fermions. The couplings d_1, \dots, d_4 are dimensionless and expected to be of $O(1)$, while Λ is the scale $\Lambda \sim 4\pi F_\pi$ below which the derivative expansion is sensible.

We emphasize the differences between a composite scalar TIMP and *fundamental* scalar dark matter considered earlier [47–49]: i) The $U(1)$ is natural, i.e. it is identified with a global symmetry (not necessarily the technibaryon one), ii) Its pNGB nature makes the DM candidate naturally light with respect to the EW scale and influences the structure of its couplings, iii) Compositeness requires the presence around the EW scale of spin-1 resonances in addition to the TIMP and the (composite) Higgs; their interplay can lead to striking collider signatures [10, 30].

III. THERMAL VERSUS ASYMMETRIC DARK MATTER

When the TIMP is a composite state made of particles charged under the EW interactions it becomes a good candidate for *asymmetric* dark matter, i.e. its present abundance is due to a relic asymmetry between the particle and its antiparticle, just as for baryons. This has been the case usually considered when discussing TC DM candidates [16, 50] since the technibaryon self-annihilation

cross-section, obtained by scaling the proton-antiproton annihilation cross-section up to the EW scale, is high enough to essentially erase any symmetric thermal relic abundance. Hence an asymmetry between technibaryons and anti-technibaryons is invoked, especially as this can be generated quite naturally in the same manner as for baryons. However, scaling up the proton-antiproton annihilation cross-section is not applicable to generic TIMPs, in particular not to pNGBs, hence they may have an interesting *symmetric* (thermal) relic abundance.

Let us solve for the thermal relic abundance of TIMPs ϕ with singlet constituents using the Boltzman continuity equation [51, 52]:

$$\frac{d}{dt}(n_\phi R^3) = -\langle \sigma_{\text{ann}} v \rangle \left[n_\phi^2 - (n_\phi^{\text{eq}})^2 \right] R^3, \quad (3)$$

where R is the cosmological scale-factor, n_ϕ the TIMP number density and σ_{ann} the TIMP-antiTIMP annihilation cross-section (given in Appendix A along with the relevant interaction vertices). From the Lagrangian (2) we see that annihilations proceed via the (composite) Higgs into SM fermions and gauge bosons pairs, as well as into a pair of (composite) Higgs particles. As discussed in Refs.[53–55], we can rewrite the continuity equation (3) in terms of the dimensionless quantities $Y \equiv n_\phi/s$, $Y^{\text{eq}} \equiv n_\phi^{\text{eq}}/s$, and $x \equiv m_\phi/T$, where $s \equiv g_s T^3$ is the specific entropy determining the value of the adiabat RT :

$$\frac{dY}{dx} = \lambda x^{-2} [(Y^{\text{eq}})^2 - Y^2], \quad (4)$$

$$\text{where, } \lambda \equiv \left(\frac{g_s^4}{180\pi} \right)^{1/6} m_\phi m_P \langle \sigma_{\text{ann}} v \rangle g_\rho^{1/2},$$

and $g_\rho \equiv \rho/T^4$ counts the number of relativistic degrees of freedom contributing to the energy density, which determines the Hubble expansion rate \dot{R}/R . The values of $g_\rho(T)$ and $g_s(T)$ have been computed in the SM [56] and are modified to account for the additional particle content of TC models.

In the hot early universe, the particle abundance initially tracks its equilibrium value but when the temperature falls below its mass and it becomes non-relativistic, its equilibrium abundance falls exponentially due to the Boltzmann factor. Hence so does the annihilation rate, eventually becoming sufficiently small that the (comoving) particle abundance becomes constant. Defining the parameter $\Delta \equiv (Y - Y^{\text{eq}})/Y^{\text{eq}}$, the freeze-out temperature is given by [53]:

$$\begin{aligned} x_{\text{fr}} = & \frac{1}{b_s} \ln [\Delta_{\text{fr}}(2 + \Delta_{\text{fr}})\delta_s] - \frac{1}{2b_s} \ln \left[\frac{1}{b_s} \ln(\Delta_{\text{fr}}(2 + \Delta_{\text{fr}})\delta_s) \right] \\ \text{where, } & b_s \equiv \left(\frac{2\pi^2 g_s}{45} \right)^{1/3}, \quad \delta_s = \frac{g}{(2\pi)^{3/2}} b_s^{-5/2} \lambda, \end{aligned} \quad (5)$$

and g counts the internal degrees of freedom, e.g. $g = 2$ for the TIMP. This gives a good match to the exact numerical solution of Eq.(4) for the choice $\Delta_{\text{fr}} = 1.5$ which corresponds to the epoch when the annihilation

rate, $n_\phi^{\text{eq}} \langle \sigma_{\text{ann}} v \rangle$, equals the logarithmic rate of change of the particle abundance itself: $d \ln n^{\text{eq}} / dt = x_{\text{fr}} \dot{R} / R$ [51]. Note that the usual criterion of equating the annihilation rate to the Hubble expansion rate \dot{R} / R would give an *erroneous* answer when there is an asymmetry [53].

We calculate the TIMP freeze out parameter x_{fr} as a function of the TIMP mass m_ϕ taking $\Lambda = 1$ TeV, for three values of the (composite) Higgs mass $m_H = 250, 500, 1000$ GeV. We also take the dimensionless effective couplings to the (composite) Higgs to be of $\mathcal{O}(1)$ and define $d_{12} \equiv d_1 + d_2$, $d_{34} \equiv d_3 + d_4$, since at low energies the d_1 and d_2 terms contribute very nearly equally, as do the d_3 and d_4 terms. There are spikes in x_{fr} at the (composite) Higgs resonance when $2m_\phi = m_H$, however the simple approximation above is not reliable near such a resonance [57] and we must then solve the full continuity equation including the (composite) Higgs width. We do this using the programme `MicrOMEGAS` [58–60] which computes the full annihilation cross-section of the model using `CalcHEP` [61]. We also use `LanHEP` [62] for the model implementation.

After freeze-out, only annihilations are important since the temperature is now too low for the inverse creations to proceed; the asymptotic abundance is then:

$$Y_\infty \equiv Y(t \rightarrow \infty) \sim \frac{x_{\text{fr}}}{\lambda_{\text{fr}}} . \quad (6)$$

The resulting cosmological energy density of relic TIMPs is shown in Fig. 1. We have checked explicitly with the numerical code that the contributions from d_1 and d_2 terms are (very nearly) identical, as are the contributions from d_3 and d_4 terms.

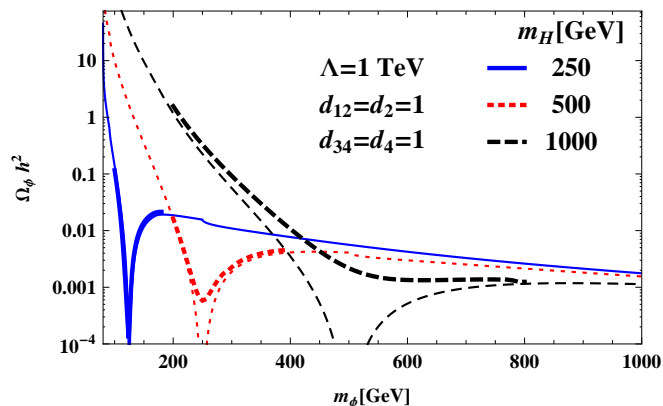


FIG. 1: The relic TIMP (ϕ) abundance vs. its mass. The thick lines show the `MicrOMEGAS` computation taking into account the (composite) Higgs decay width.

Fig. 2 shows the region in the (composite) Higgs versus TIMP mass plane where the TIMP relic abundance matches the DM abundance $\Omega h^2 = 0.11 \pm 0.01$ (2σ) inferred from WMAP-7 [63].

From Figs. 1 and 2 we observe first that the relic energy density drops significantly for $m_\phi \sim 2m_H$ as expected

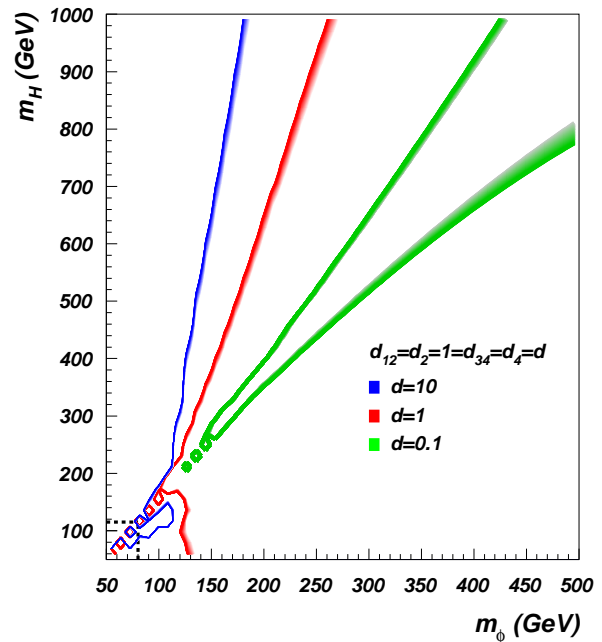


FIG. 2: Regions corresponding to $\Omega h^2 = 0.11 \pm 0.01$ for the relic TIMP (ϕ) abundance in the (composite) Higgs vs. TIMP mass plane. The dashed box shows that given $m_H > 115$ GeV, we require $m_\phi > m_W$ for TIMPs to be dark matter.

(because ϕ can then decay resonantly through the Higgs) and, second, that if m_H is greater than about 115 GeV then for TIMPs to be dark matter requires $m_\phi > m_W$.

As discussed below, in the presence of an asymmetry the total relic abundance always increases relative to the same model with no asymmetry, so m_W provides a general *lower* bound for the mass of the pNGB TIMPs we consider. It follows that in the interesting region $m_W \lesssim m_\phi \lesssim 1$ TeV, *symmetric* relic TIMPs with singlet constituents could make up a significant fraction of the dark matter in the universe. However when the TIMP is heavier than about a TeV, the strength of the interaction is similar to that of an ordinary (scalar) technibaryon, and a relic abundance large enough to account for dark matter now does require an initial *asymmetry* similar to that of baryons as discussed earlier [16, 17]. We note that recently a different type of QCD-like pions (which do not carry a $U(1)$ quantum number) were also considered as dark matter candidates [64, 65].

A. Adding an asymmetry

To study the relic abundance in the presence of both a thermal component and an initial asymmetry we follow Ref.[53] and define the asymmetry as $\alpha = (Y_+ - Y_-)/2$ where Y_\pm are the abundances of the majority and minority species (TIMP and anti-TIMP) respectively. The

abundance in thermal and chemical equilibrium is:

$$Y_-^{\text{eq}} = e^{-\mu/T} Y^{\text{eq}} \sim e^{-\mu/T} g \left(\frac{x}{2\pi b_s} \right)^{3/2} e^{-b_s x}, \quad (7)$$

where μ is the chemical potential. The continuity equation in the presence of an asymmetry is [53]:

$$\frac{dY_-}{dx} = \lambda x^{-2} [Y_-^{\text{eq}}(Y_-^{\text{eq}} + 2\alpha) - Y_-(Y_- + 2\alpha)], \quad (8)$$

and the total asymptotic abundance of TIMPs and anti-TIMPs is:

$$\Omega_\phi h^2 = 5.5 \times 10^8 (Y_{-\infty} + \alpha) \frac{m_\phi}{\text{GeV}}. \quad (9)$$

In Fig. 3 we show the minority species abundance Y_- as a function of $x \equiv m_\phi/T$ for $m_\phi = 100$ GeV and $\alpha = 9.8 \times 10^{-9}, 5.6 \times 10^{-10}, 10^{-11}$, taking the Higgs mass to be $m_H = 250, 500, 1000$ GeV.

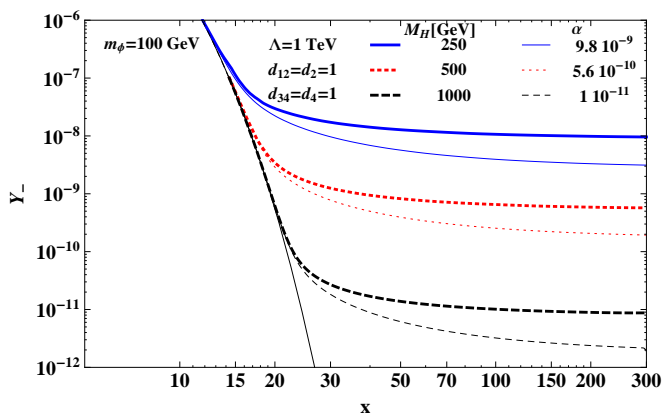


FIG. 3: TIMP (ϕ) abundance when there is no asymmetry (thick lines), compared with the abundance of the *minority* species Y_- (thin lines) when an asymmetry α is present.

We see from the figure that the *symmetric* component of the relic abundance is $\sim 10\%$ of the asymmetric component, when the asymmetry is comparable to the would-be symmetric abundance (in the absence of an asymmetry). In the limit where $\alpha \ll Y_\infty$, the symmetric component is unchanged and the asymmetry provides a small addition to the total relic abundance. When $\alpha \gtrsim Y_\infty$, the abundance of the minority species is exponentially suppressed in α and provides a negligible addition to the asymmetric component. Adding an asymmetry will always *increase* the relic abundance relative to its value in the same model in the absence of an asymmetry. This implies a non-trivial constraint on the mass of TIMPs with uncharged constituents discussed above, such as appear in e.g. the UMT model. The constraint is non-trivial since such states would evade direct detection at colliders unless the (composite) Higgs is very light [30], as well as the direct detection experiments discussed below.

Fig. 4 shows the contour in the $m_H - m_\phi$ plane where

the relic abundance of ϕ agrees with the DM abundance inferred from WMAP-7 [63] for a fixed value of the d coefficients. Just as in Figs. 1 and 2 we observe that if m_H is greater than ~ 115 GeV we require $m_\phi > m_W$ to avoid an excessive TIMP relic abundance. However, due to the asymmetry, for TIMP masses above m_W there is now a much broader range of m_H and m_ϕ where the relic abundance of ϕ matches the observed DM abundance.

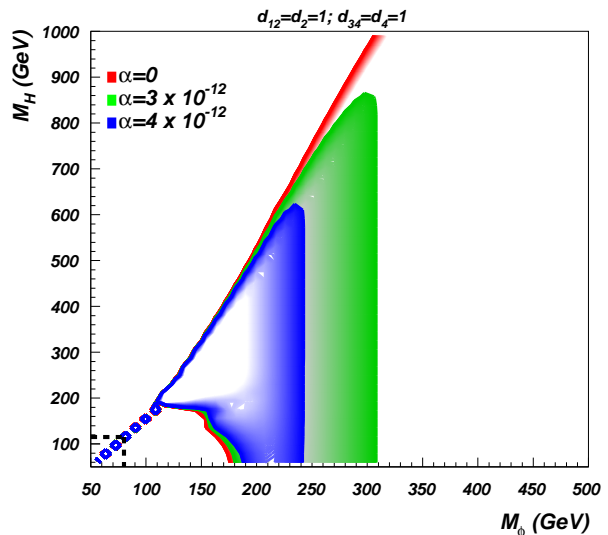


FIG. 4: Regions in the (composite) Higgs versus TIMP mass plane corresponding to $\Omega h^2 = 0.11 \pm 0.01$ for the TIMP (ϕ) relic abundance, for different values of the relic asymmetry α . The dashed box shows that given $m_H > 115$ GeV, we require $m_\phi > m_W$ for TIMPs to be dark matter.

B. TIMPs with charged constituents

We consider now pNGB TIMPs with charged constituents of the form $T \sim UD$ arising from the TC sector carrying EW interactions (see Eq. 1). These states carry an $U(1)$ quantum number which makes them stable and it is natural to identify this global symmetry with the technibaryon number. Such particles arise generally in TC models with the technifermions transforming in either real or pseudo-real representations of the gauge group. Explicit examples are furnished again in the UMT scheme in which the composite T is a SM singlet and the ‘orthogonal minimal technicolor’ (OMT) model in which the T state is the isospin-0 component of a complex triplet [10].

We demonstrate that similarly to the case of TIMPs with neutral constituents, TIMPs with charged constituents have a significant symmetric component in only a small region of parameter space. However, as opposed to the TIMPs with SM neutral constituents this region is essentially independent of the parameters of the (composite) Higgs interactions. In addition to the interactions

investigated above, the scalar TIMPs containing charged constituents will also have an effective interaction with the photon, due to a non-zero electromagnetic charge radius of T [18, 30]:

$$\mathcal{L}_B = ie \frac{d_B}{\Lambda^2} T^* \overleftrightarrow{\partial}_\mu T \partial_\nu F^{\mu\nu} . \quad (10)$$

The corresponding charge radius of the TIMP is $r_T \sim \sqrt{d_B}/\Lambda$. For our choice $\Lambda = 1$ TeV we consider the range $|d_B| = 0$ to 0.3 while for a higher cut-off Λ , a larger $d_B \sim O(1)$ would be expected.

In case of the TIMP T there are also contact interactions with two SM vector bosons V , arising from the kinetic term of the chiral Lagrangian, which can significantly affect the symmetric relic density. In general these can be written as

$$L_{VV} = \frac{1}{2} T^* T V_\mu V^\mu \text{Tr} \left[[\Lambda_S, [\Lambda_S, X_T]] X_{T^*} - [\Lambda_S, [\Lambda_S, X_T]] X_{T^*} \right], \quad (11)$$

where X_T is the generator of the broken (techni) flavor direction corresponding to the TIMP and Λ_S are the, appropriately normalized, EW generators imbedded in the TC chiral group [68–70]. The resulting $TTWW$ and $TTZZ$ contact interactions (assuming that the EW symmetry is broken already) are:

$$L_{WW,ZZ} = -\frac{T^* T}{2} \text{Tr} [d_W W_\mu W^\mu + d_Z Z_\mu Z^\mu], \quad (12)$$

with $d_W = g^2$ and $d_Z = (g^2 + g'^2)/2$ for the TIMPs T of both the UMT and the OMT models.

In Fig. 5 we display the effect of the W and Z contact interactions, as well as of the charge radius interaction, on the thermal relic abundance. It is seen that for m_T significantly below m_W , the interactions in Eq.(10) do affect TIMP annihilations significantly, even so the TIMP relic abundance is too large. As m_T increases towards m_W , annihilations due to the $TTVV$ interactions in Eq.(12) begin to dominate and reduce the TIMP relic abundance to the observationally acceptable level only when the TIMP is a few GeV lighter than the W .

Again, once we include an asymmetry, the range of TIMP masses where a cosmologically acceptable *symmetric* relic abundance is achieved, can be much broader. This is demonstrated in Fig. 6 which shows the contours of Ωh^2 for different values of the asymmetry and m_T . There is a cross-over in the small TIMP mass region mentioned above, from just below m_W where the relic abundance is dominated by the asymmetry, to just above m_W where it is dominated by the symmetric component.

IV. DIRECT DETECTION

Direct detection of the TIMPs ϕ with SM singlet constituents will be challenging. The exchange of the (com-

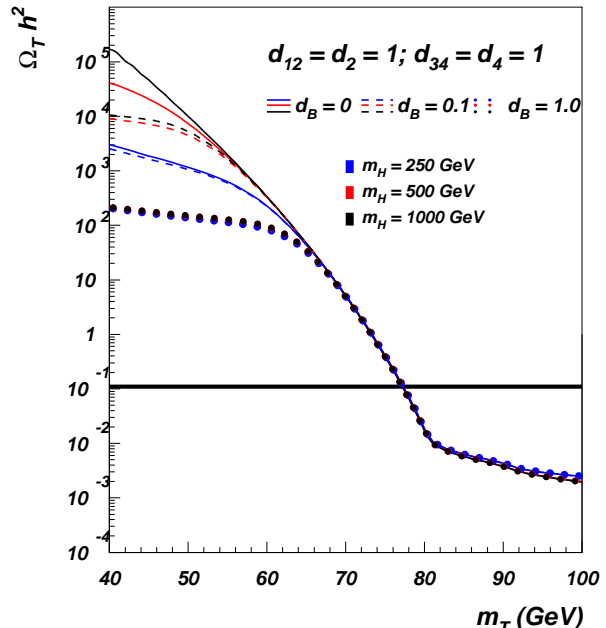


FIG. 5: The TIMP (T) relic energy density as a function of its mass when W and Z contact interactions are present, calculated taking into account their off-shell decays. The horizontal band corresponds to $\Omega h^2 = 0.11 \pm 0.01$.

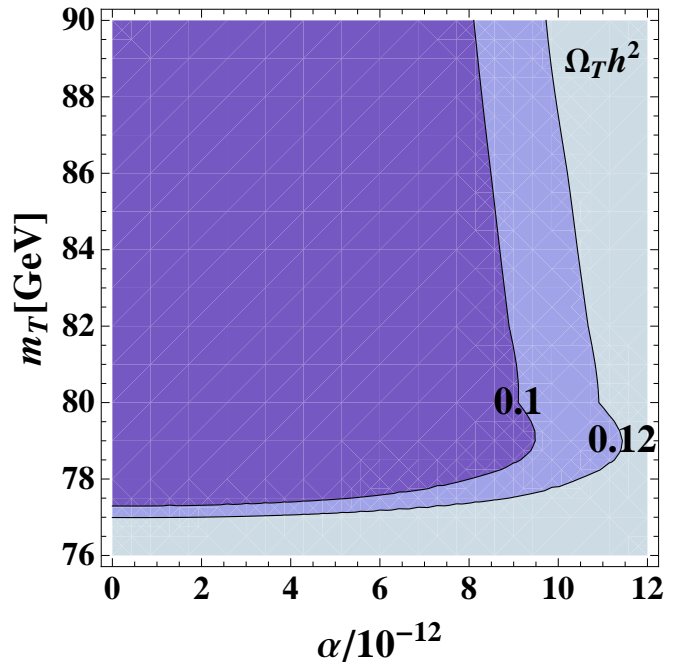


FIG. 6: The region in the asymmetry (α) vs. TIMP (T) mass plane which yields the marked relic energy density (consistent with WMAP) when W and Z contact interactions are present.

posite) Higgs leading to a scattering cross-section on nuclei is the most relevant interaction here, and we will assume that the (composite) Higgs couples to SM fermions with ordinary Yukawa couplings. (In fact this represents an upper bound and so the actual cross-section could be

lower). Again, since the TIMP is a pNGB the couplings to the Higgs are suppressed at low masses. The TIMP nucleon scattering cross-section from the (composite) Higgs exchange is given by:

$$\sigma_{\text{nucleon}}^H = \frac{\mu^2}{2\pi} \left[\frac{d_H f m_N}{m_H^2 m_\phi v} \right]^2, \quad d_H = (d_1 + d_2) \frac{m_\phi^2}{\Lambda}, \quad (13)$$

where μ is the nucleon-TIMP reduced mass, v the electroweak vev and f parameterizes the (composite) Higgs-nucleon coupling. We refer to Refs.[72, 73] for recent discussions on the strange quark contribution to f which we take to be $f = 0.3$.

For TIMPs T with charged constituents there is an additional contribution to the scattering on nuclei via the charge radius operator [18, 30]

$$\sigma_p^\gamma = \frac{\mu^2}{4\pi} \left[\frac{8\pi \alpha d_B}{\Lambda^2} \right]^2. \quad (14)$$

To take into account the possible interference between the composite Higgs and photon exchange [30] we write an averaged scalar cross-section per nucleon as

$$\sigma_{\text{nucleon}} \equiv \frac{\mu^2}{4\pi A^2} (f_p Z + f_n (A - Z))^2 \quad (15)$$

$$\text{where: } f_n = -\frac{\sqrt{2} d_H f m_N}{m_H^2 m_\phi v}, \quad f_p = f_n + \frac{8\pi \alpha d_B}{\Lambda^2}.$$

The direct detection cross-section per nucleon as a function of the TIMP mass is shown in Fig. 7, where we also indicate, (following Ref.[74]) the limits from the CDMS II [76] and XENON-100 [77] experiments.

For Higgs exchange only ($d_B = 0$) the direct detection cross-section *increases* with TIMP mass since the TIMPs are pNGBs (*c.f.* Ref. [30] where the TIMPs were not derivatively coupled to the (composite) Higgs). However, the charge radius interaction can significantly alter the cross-section, by up to 2 orders of magnitude for $|d_B| \simeq 0.3$, thus greatly affecting the discovery potential of direct detection experiments. For example, for $d_B = -0.3$ and $d_{12} = 3$ the signals from the TIMP T with SM charged constituents would have been observed already by CDMS II and XENON-100. On the other hand, for *positive* values of d_B , there is a destructive interference between (composite) Higgs and photon exchange, lowering the cross section to 10^{-47} cm^2 at $m_T \simeq 200 \text{ GeV}$ for a particular choice of the parameters.

Since the direct detection rate depends strongly on the (composite) Higgs mass, we present in Fig. 8 results in the $(M_H - m_T)$ plane for different values of the d_B parameter. The figure also shows the exclusion limits from the XENON-10 [75], CDMS II [76] and XENON-100 [77] experiments. One can see that for $d_B = 0$ and $d_{12} = 3$ (top frame), XENON-100 and CDMS II can cover essentially the whole range of m_T for M_H below 150 GeV where the cross-section always exceeds 10^{-42} cm^2 . Our results trivially scale as d_{12}^2 for $d_B = 0$. Negative $d_B = -0.3$ signif-

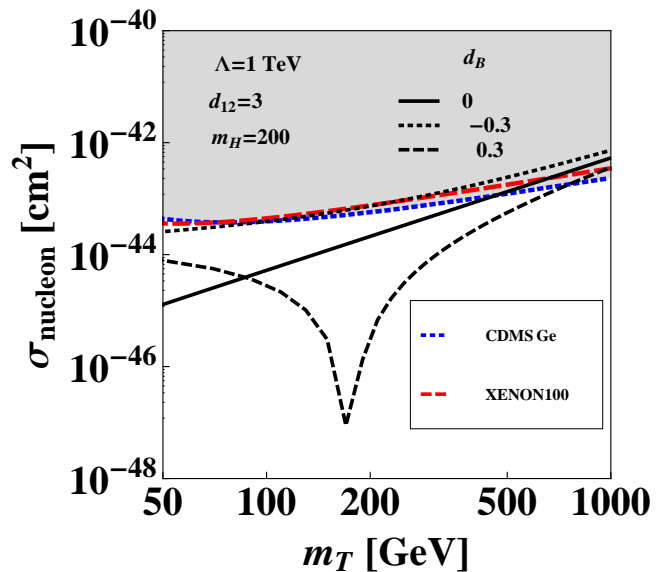


FIG. 7: Direct detection cross-section (per nucleon) for TIMP scattering off nuclei. The full line is for Higgs exchange only (with $m_H = 200 \text{ GeV}$) while the short- and long-dashed lines show the additional effect of the charge radius operator (with $d_B = -0.3$ and $d_B = +0.3$ respectively). The shaded region is experimentally excluded.

icantly enhances the cross-section (middle frame) while positive $d_B = 0.3$ (bottom frame) brings the negative interference effect into play, resulting in a deep valley.

V. CONCLUSIONS

We have shown that models of dynamical EW symmetry breaking can provide symmetric (thermal) DM, as well as asymmetric (non-thermal) DM. This is true in particular for *partially gauged technicolor* [6, 40] which can satisfy constraints from EW precision measurements.

From our analysis we conclude that for pNGB TIMPs:

- 1) The TIMP cannot be significantly lighter than the W if its relic abundance is to be acceptable, unless the (composite) Higgs mass is below 115 GeV — this holds whether it is symmetric, asymmetric or a combination.
- 2) If the TIMP is made of constituents charged under EW interactions, it can be symmetric DM only in a narrow mass range close to m_W . Above this mass an initial asymmetry is required for TIMPs to be dark matter.
- 3) If the constituents of the TIMP are neutral with respect to the EW interactions then it can be symmetric dark matter for a range of masses tied to the (composite) Higgs mass. This does not exclude the possibility that it has an asymmetry as well.
- 4) Direct detection of light pNGB TIMPs with neutral constituents is challenging due to its mass suppressed couplings to the (composite) Higgs. However, for TIMPs with charged constituents there is an addi-

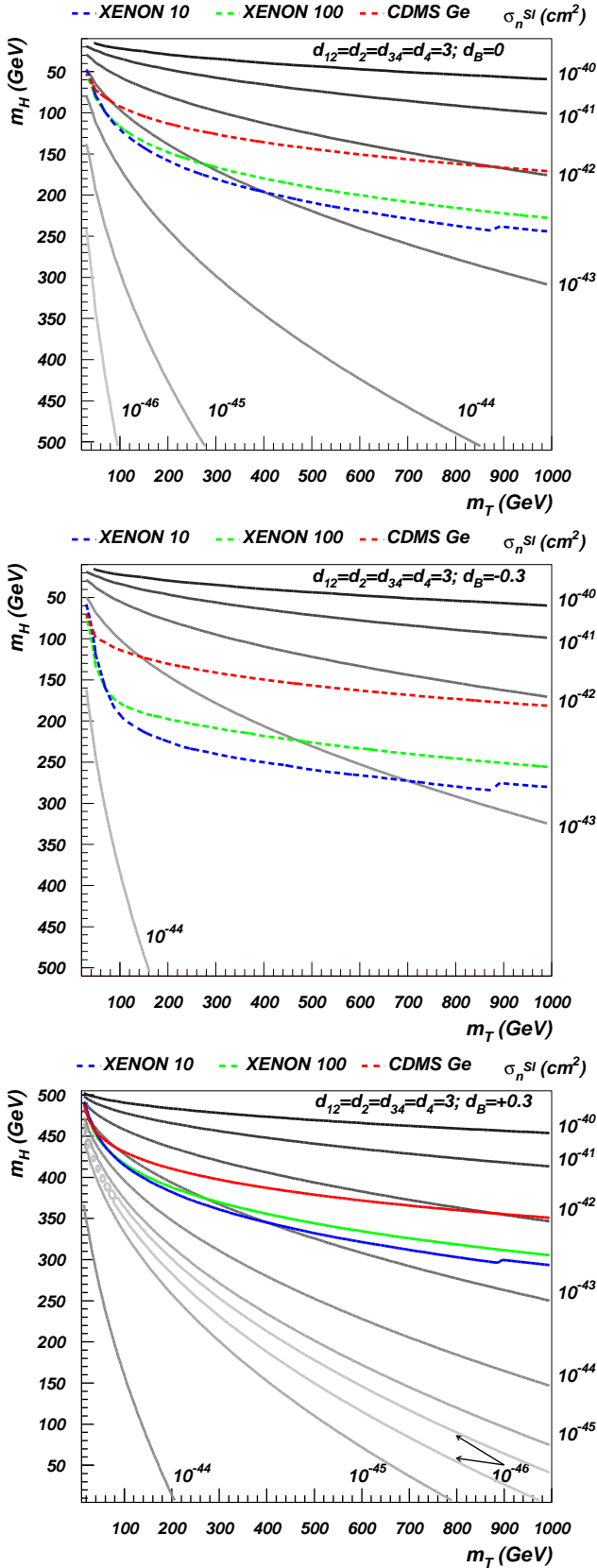


FIG. 8: Contours of the direct detection cross-section (per nucleon) for TIMP scattering off nuclei in the TIMP mass vs. (composite) Higgs mass plane. The top, middle and bottom frames are for $d_B = 0, -0.3, +0.3$ respectively. The dashed curves show the upper limits from CDMS II (red), XENON-10 (blue) and XENON-100 (green).

tional charge radius interaction which, if sizeable, can bring such TIMPs within the reach of current nuclear recoil detection experiments.

Both types of TIMPs considered here – with charged or neutral constituents – can co-exist and contribute to the dark matter (as in e.g. the UMT model [8]). These models provide interesting signals for direct dark matter detection experiments which are already sensitive enough to exclude TIMPs in certain regions of parameter space or even discover them in the near future.

Acknowledgements

We wish to thank A. Pukhov for providing a modified version of MicrOMEGAs (including an asymmetry in the solution of the continuity equation), and C. McCabe for providing fits to direct detection experimental data. MTF acknowledges a VKR Foundation Fellowship. SS acknowledges support by the EU Marie Curie Network “UniverseNet” (HPRN-CT-2006-035863).

Appendix A: Annihilation cross-section

The relevant vertex factors at low energies (if we keep only the light (composite) Higgs in the spectrum) are:

$$\begin{aligned} \phi^* \phi H &: i \left(\frac{p_{\phi^*} p_{\phi}}{\Lambda} d_1 + d_2 \frac{m_{\phi}^2}{\Lambda} \right) \rightarrow i d_{12} \frac{m_{\phi}^2}{\Lambda} \\ \phi^* \phi H H &: i \left(\frac{p_{\phi^*} p_{\phi}}{\Lambda^2} d_3 + d_4 \frac{m_{\phi}^2}{\Lambda^2} \right) \rightarrow i d_{34} \frac{m_{\phi}^2}{\Lambda^2} \quad (\text{A1}) \end{aligned}$$

where $d_{12} = d_1 + d_2$ and $d_{34} = d_3 + d_4$ are the only independent parameters at low energies. Hence the (composite) Higgs mediated contributions to the cms annihilation cross-section $\langle \sigma v_{\text{rel}} \rangle$ in the limit $v_{\text{rel}} \rightarrow 0$ are:

$\phi \phi^* \rightarrow H H$:

$$\frac{1}{64\pi m_{\phi}^2} \left[\frac{3d_{12} m_H^2 m_{\phi}^2}{v\Lambda (4m_{\phi}^2 - m_H^2)} - \frac{2d_{12}^2 m_{\phi}^4}{\Lambda^2 (m_H^2 - 2m_{\phi}^2)} + \frac{d_{34} m_{\phi}^2}{\Lambda^2} \right]^2 \times \left(1 - \frac{m_H^2}{m_{\phi}^2} \right)^{1/2} \quad (\text{A2})$$

$\phi \phi^* \rightarrow W^+ W^-$:

$$2 \left[1 + \frac{1}{2} \left(1 - \frac{2m_{\phi}^2}{m_W^2} \right)^2 \right] \frac{d_{12}^2 m_{\phi}^2 m_W^4}{8\pi v^2 \Lambda^2 \left[(4m_{\phi}^2 - m_h^2)^2 + m_h^2 \Gamma_h^2 \right]} \times \left(1 - \frac{m_W^2}{m_{\phi}^2} \right)^{1/2} \quad (\text{A3})$$

$\phi\phi^* \rightarrow ZZ$:

$$2 \left[1 + \frac{1}{2} \left(1 - \frac{2m_\phi^2}{m_Z^2} \right)^2 \right] \frac{d_{12}^2 m_\phi^2 m_Z^4}{16\pi v^2 \Lambda^2 \left[(4m_\phi^2 - m_h^2)^2 + m_h^2 \Gamma_h^2 \right]} \times \left(1 - \frac{m_Z^2}{m_\phi^2} \right)^{1/2} \quad (\text{A4})$$

$\phi\phi^* \rightarrow \bar{f}f$:

$$\frac{c_f}{4\pi v^2 \Lambda^2} \frac{\lambda_f^2 d_{12}^2 m_\phi^4}{\left[(4m_\phi^2 - m_h^2)^2 + m_h^2 \Gamma_h^2 \right]} \left(1 - \frac{m_f^2}{m_\phi^2} \right)^{3/2} \quad (\text{A5})$$

Here the fermion Yukawa coupling is $\lambda_f = m_f/v$ where $v \simeq 246$ GeV and m_f is the fermion mass, while $c_f = 1, 3$ for leptons and quarks respectively. The contributions from the photon mediated annihilations from the charge-radius operator are negligible and we do not include these.

We implement the Lagrangian in Eq. (2) in `CalcHEP` [61] and in `MicrOMEGAs` [59] (using the `LanHEP` module [62] to check the above implementation), in order to compute the full $2 \rightarrow 2$ annihilation cross-section including finite widths and to study the collider phenomenology.

-
- [1] S. Weinberg, Phys. Rev. D **19**, 1277 (1979).
[2] L. Susskind, Phys. Rev. D **20**, 2619 (1979).
[3] F. Sannino and K. Tuominen, Phys. Rev. D **71**, 051901 (2005).
[4] D. K. Hong, S. D. H. Hsu and F. Sannino, Phys. Lett. B **597**, 89 (2004).
[5] D. D. Dietrich, F. Sannino and K. Tuominen, Phys. Rev. D **73**, 037701 (2006).
[6] D. D. Dietrich, F. Sannino and K. Tuominen, Phys. Rev. D **72**, 055001 (2005).
[7] S. B. Gudnason, T. A. Rytto and F. Sannino, Phys. Rev. D **76**, 015005 (2007).
[8] T. A. Rytto and F. Sannino, Phys. Rev. D **78**, 115010 (2008).
[9] M. T. Frandsen, I. Masina and F. Sannino, Phys. Rev. D **81**, 035010 (2010).
[10] M. T. Frandsen and F. Sannino, Phys. Rev. D **81**, 097704 (2010).
[11] O. Antipin, M. Heikinheimo and K. Tuominen, JHEP **0910**, 018 (2009).
[12] R. Foadi, M. T. Frandsen, T. A. Rytto and F. Sannino, Phys. Rev. D **76**, 055005 (2007).
[13] A. Belyaev, R. Foadi, M. T. Frandsen, M. Jarvinen, F. Sannino and A. Pukhov, Phys. Rev. D **79**, 035006 (2009).
[14] M. Antola, M. Heikinheimo, F. Sannino and K. Tuominen, JHEP **1003**, 050 (2010).
[15] O. Antipin, M. Heikinheimo and K. Tuominen, JHEP **1007**, 052 (2010).
[16] S. Nussinov, Phys. Lett. B **165**, 55 (1985).
[17] S. M. Barr, R. S. Chivukula and E. Farhi, Phys. Lett. B **241**, 387 (1990).
[18] J. Bagnasco, M. Dine and S. D. Thomas, Phys. Lett. B **320**, 99 (1994).
[19] S. B. Gudnason, C. Kouvaris and F. Sannino, Phys. Rev. D **73**, 115003 (2006).
[20] S. B. Gudnason, C. Kouvaris and F. Sannino, Phys. Rev. D **74**, 095008 (2006).
[21] K. Kainulainen, K. Tuominen and J. Virkajarvi, Phys. Rev. D **75**, 085003 (2007).
[22] C. Kouvaris, Phys. Rev. D **76**, 015011 (2007).
[23] C. Kouvaris, Phys. Rev. D **77**, 023006 (2008).
[24] M. Y. Khlopov and C. Kouvaris, Phys. Rev. D **77**, 065002 (2008).
[25] M. Y. Khlopov and C. Kouvaris, Phys. Rev. D **78**, 065040 (2008).
[26] C. Kouvaris, Phys. Rev. D **78**, 075024 (2008).
[27] K. Belotsky, M. Khlopov and C. Kouvaris, Phys. Rev. D **79**, 083520 (2009).
[28] J. M. Cline, M. Jarvinen and F. Sannino, Phys. Rev. D **78**, 075027 (2008).
[29] E. Nardi, F. Sannino and A. Strumia, JCAP **0901**, 043 (2009).
[30] R. Foadi, M. T. Frandsen and F. Sannino, Phys. Rev. D **80**, 037702 (2009).
[31] M. Jarvinen, T. A. Rytto and F. Sannino, Phys. Lett. B **680**, 251 (2009).
[32] M. Jarvinen, C. Kouvaris and F. Sannino, Phys. Rev. D **81**, 064027 (2010).
[33] K. Kainulainen, K. Tuominen and J. Virkajarvi, JCAP **1002**, 029 (2010).
[34] K. Kainulainen, K. Tuominen and J. Virkajarvi, arXiv:1001.4936 [astro-ph.CO].
[35] M. T. Frandsen and S. Sarkar, Phys. Rev. Lett. **105**, 011301 (2010).
[36] C. Kouvaris and P. Tinyakov, arXiv:1004.0586 [astro-ph.GA].
[37] F. Sannino, arXiv:0911.0931 [hep-ph].
[38] H. S. Fukano and F. Sannino, arXiv:1005.3340 [hep-ph].
[39] R. S. Chivukula and E. H. Simmons, arXiv:1005.5727 [hep-lat].
[40] D. D. Dietrich and F. Sannino, Phys. Rev. D **75**, 085018 (2007).
[41] F. Sannino, arXiv:1006.0207 [hep-lat].
[42] F. Sannino, arXiv:1007.0254 [hep-ph].
[43] M. A. Luty and T. Okui, JHEP **0609**, 070 (2006).
[44] J. Galloway, J. A. Evans, M. A. Luty and R. A. Tacchi, arXiv:1001.1361 [hep-ph].
[45] E. Eichten and K. D. Lane, Phys. Lett. B **90**, 125 (1980).
[46] T. Appelquist and R. Shrock, Phys. Lett. B **548**, 204 (2002).
[47] J. McDonald, Phys. Rev. D **50**, 3637 (1994).
[48] M. Cirelli, N. Fornengo and A. Strumia, Nucl. Phys. B **753**, 178 (2006).
[49] S. Andreas, T. Hambye and M. H. G. Tytgat, JCAP **0810**, 034 (2008).
[50] R. S. Chivukula and T. P. Walker, Nucl. Phys. B **329**, 445 (1990).
[51] B. W. Lee and S. Weinberg, Phys. Rev. Lett. **39**, 165 (1977).

- [52] M. I. Vysotsky, A. D. Dolgov and Y. B. Zeldovich, JETP Lett. **26**, 188 (1977).
- [53] K. Griest and D. Seckel, Nucl. Phys. B **283**, 681 (1987) [Erratum-ibid. B **296**, 1034 (1988)].
- [54] P. Gondolo and G. Gelmini, Nucl. Phys. B **360**, 145 (1991).
- [55] S. A. Abel, S. Sarkar and I. B. Whittingham, Nucl. Phys. B **392**, 83 (1993).
- [56] M. Srednicki, R. Watkins and K. A. Olive, Nucl. Phys. B **310**, 693 (1988).
- [57] K. Griest and D. Seckel, Phys. Rev. D **43**, 3191 (1991).
- [58] G. Belanger, F. Boudjema, A. Pukhov and A. Semenov, Comput. Phys. Commun. **149**, 103 (2002).
- [59] G. Belanger, F. Boudjema, A. Pukhov and A. Semenov, Comput. Phys. Commun. **180**, 747 (2009).
- [60] G. Belanger, F. Boudjema, P. Brun, A. Pukhov, S. Rosier-Lees, P. Salati and A. Semenov, arXiv:1004.1092 [hep-ph].
- [61] A. Pukhov, arXiv:hep-ph/0412191.
- [62] A. Semenov, Comput. Phys. Commun. **180**, 431 (2009).
- [63] D. Larson *et al.*, arXiv:1001.4635 [astro-ph.CO].
- [64] T. Hur, D. W. Jung, P. Ko and J. Y. Lee, arXiv:0709.1218 [hep-ph].
- [65] Y. Bai and R. J. Hill, arXiv:1005.0008 [hep-ph].
- [66] A. Doff, A. A. Natale and P. S. Rodrigues da Silva, Phys. Rev. D **77**, 075012 (2008).
- [67] A. Doff, A. A. Natale and P. S. Rodrigues da Silva, Phys. Rev. D **80**, 055005 (2009).
- [68] J. Preskill, Nucl. Phys. B **177**, 21 (1981).
- [69] M. E. Peskin, Nucl. Phys. B **175**, 197 (1980).
- [70] S. Chadha and M. E. Peskin, Nucl. Phys. B **185**, 61 (1981).
- [71] D. D. Dietrich and M. Jarvinen, Phys. Rev. D **79**, 057903 (2009).
- [72] H. Ohki *et al.*, Phys. Rev. D **78**, 054502 (2008).
- [73] J. Giedt, A. W. Thomas and R. D. Young, Phys. Rev. Lett. **103**, 201802 (2009).
- [74] C. McCabe, arXiv:1005.0579 [hep-ph].
- [75] J. Angle *et al.* [XENON Collaboration], Phys. Rev. Lett. **100**, 021303 (2008).
- [76] Z. Ahmed *et al.* [The CDMS-II Collaboration], arXiv:0912.3592 [astro-ph.CO].
- [77] E. Aprile *et al.* [XENON100 Collaboration], arXiv:1005.0380 [astro-ph.CO].